Development of a Radio-Frequency Generator for RF Ion Thrusters

IEPC-2015-289／ISTS-2015-b-289

Presented at Joint Conference of 30th International Symposium on Space Technology and Science,
34th International Electric Propulsion Conference and 6th Nano-satellite Symposium
Hyogo-Kobe, Japan
July 4–10, 2015

J. Simon* and U. Probst†
University of Applied Sciences, Giessen, 35390, Germany

P. J. Klar‡
University of Giessen, Giessen, 35392, Germany

Abstract: To ensure the successful operation of a thruster using inductively-coupled plasmas (e.g. radio-frequency ion thrusters (RIT)), a high efficiency and high performance radio-frequency (RF) power supply is crucial. For this purpose, the supply needs to guarantee highly efficient RF signal generation and transfer to the thruster coil and furthermore an optimal power coupling between coil and plasma.

In this paper we propose a high efficiency, high performance approach of generating RF power by using a resonant converter design. Due to a compensation of the load's inductance, resonant switching behavior becomes possible and thus, switching losses can be significantly reduced. The drive signals of the power semiconductors are generated by a switching frequency-adapting, load-controlled algorithm, which keeps up a quasi-resonant state. Due to high-speed tracking of the resonance frequency and phase, RF generation can be adjusted to altered load conditions within a few RF-cycles. A digital FPGA-based implementation guarantees a precise period determination and control signal generation, since the programmed control-algorithm is executed in hardware. The proper functioning of the developed radio-frequency generator (RFG) concept is verified through performance mappings, recorded when supplying a RIM-4 RF ion thruster developed at the University of Giessen.

In the long run, this RFG concept shall be employed for driving RIT more efficiently.

Nomenclature

c	= speed of light ($\mathrm{m\,s^{-1}}$)	n_e	= electron density
C	= capacitance	Q_L	= factor of quality
f_0	= resonance frequency ($\mathrm{s^{-1}}$)	R	= resistance
f_s	= switching frequency	T_e	= electron temperature
$i_{\mathrm{zero-sig}}$	= current measurement signal	T_k	= determined periodic-time
$\tilde{I}_\mathrm{coil}$	= complex current phasor	T_Lead	= dead time compensation
λ_RF	= RF-signal wave length (m)	T_s	= switching period
l_sl	= length of RF supply line (m)	$v_{\mathrm{GS\ T+}}$	= drive signal of $\mathrm{T_+}$
L	= inductance	$v_{\mathrm{GS\ T-}}$	= drive signal of $\mathrm{T_-}$
M	= mutual inductance	v_RF	= RF-signal propagation speed ($\mathrm{m\,s^{-1}}$)
n_0	= neutral gas density	$\tilde{V}_\mathrm{coil}$	= complex voltage phasor

*Research Assistant, Department of Electrical Engineering, jens.simon@ei.thm.de
†Professor, Department of Electrical Engineering, uwe.probst@ei.thm.de
‡Professor, Institute of Experimental Physics I, Peter.J.Klar@exp1.physik.uni-giessen.de

I. Introduction

Inductively coupled plasmas within radio-frequency (RF) ion thrusters have been used commercially for the last 20 years.[1] As those thrusters can also be used as conventional ion sources, their utilization is not restricted to space applications. In addition, they offer, due to their high energy efficiency and scalability, a wide range of terrestrial applications in the area of material processing.[2]

Especially the gridded RF ion thrusters (RIT)—developed by H. Loeb at the University of Giessen in the 1960s[3]—provide further advantages due to the separation of the plasma generation process by electrodeless discharge and the thrust generation process by electrostatic ion extraction.

Together with Giessen University our research group works on optimizing the RITs' overall efficiency by developing models describing the RF thrusters impedance[4] and electromagnetic interference (EMI)[5] as well as peripheral devices such as beam-current controllers (BCC)[6] and RF power supplies.

To supply the inductively coupled plasma discharge needed for thrust generation a radio-frequency generator (RFG) is required. In contrast to terrestrial applications—where the RFG may consume power up to several kilowatts with low effectiveness—electrical efficiency plays a major role in space applications. Therefore, the RF power supply needs to guarantee highly efficient RF signal generation and transfer to the thruster coil as well as an optimal power coupling between coil and plasma.

In this paper, we introduce a new concept for a high efficiency, high performance approach of generating RF power. By implementing a switching frequency-adapting, load-controlled algorithm, the generator losses can be minimized by applying resonant switching behavior. Furthermore, fast and reliable tracking of the maximum power point of operation is secured by choosing a digital, FPGA-based implementation of the control algorithm.

The next sections give background information on the theories and explain the RFG's circuit and control concept. The designed hardware assembly is shown as well as performance measurements, supplying a RIM-4 RF ion thruster developed at the University of Giessen.

II. Theory and Principle of Operation

To ensure the efficient operation of a RIT, a low-loss RF generation with extremely fast adaption with respect to changes of the plasma load is crucial. Therefore, only generator concepts based on a switch-mode power supply topology are worth to be considered.

The required frequency for supplying RF ion thrusters depends on the geometry of the coil and discharge vessel as well as on the inner plasma parameters n_0, n_e, and T_e. Though an increasing frequency leads to an improved inductive coupling, the coil resistance rises and the penetration depth of the electromagnetic field inside the plasma decreases due to the skin-effect. Thus, for established RIT geometries, an optimum can be found within the single-digit MHz-range. Hence, switching losses represent a very high proportion of the overall losses in RF signal generation and measures of reducing switching losses are desirable.

To achieve an optimal power coupling between thruster coil and plasma, a sinusoidal load current is mandatory. On that score—and to be able to minimize switching losses—a resonant converter topology is chosen.[7]

Moreover, a switching frequency-adapting, load controlled algorithm, which takes impedance changes of the inductively coupled plasma into account and thus ensures an optimal energy flow into the load, is designed. By means of a digital implementation of the algorithm, the control system is able to consistently match the generator to high dynamic load conditions within a few RF cycles. Thus, it prevents significant decrease of output power during the matching process.

A. Circuit Design Concept

From the electrical point of view, an inductive discharge—as it appears in RF ion thrusters—can typically be modeled by a transformer, shown in Fig. 1(a). The primary represents the thruster coil, while the secondary depends on the inner plasma parameters n_0, n_e, and T_e. Following Ref. 8, this model can easily be simplified into its series equivalent circuit, shown in Fig. 1(b). In this circuit $R_\mathrm{c+pl}$ and $L_\mathrm{c+pl}$ represent the thruster coil in conjunction with the plasma and form an ohmic-inductive load. Therefore, changes of the plasma affect both, the ohmic and the inductive component.

The resonant converter concept used is shown in Fig. 2. The generator is supplied by the DC-voltage V_DC and consists of a half-bridge, loaded with a series-resonant circuit.

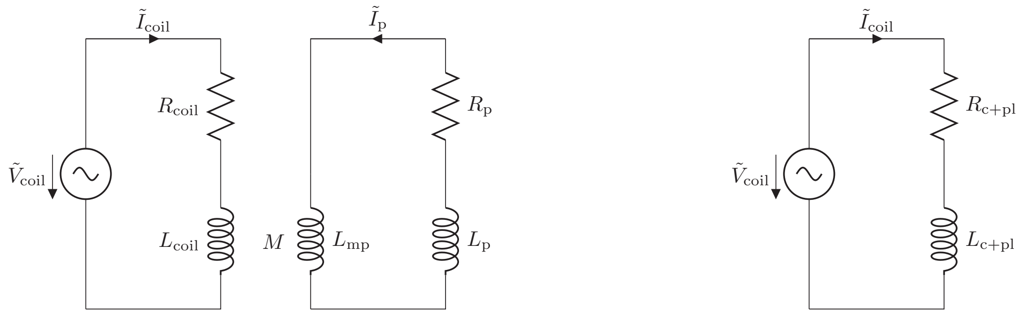

(a) Transformer model (b) Series equivalent circuit model

Figure 1. Modeling of the inductive discharge

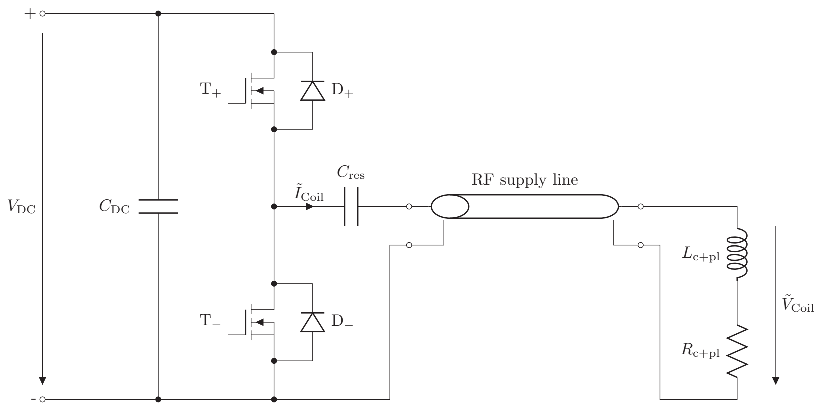

Figure 2. Circuit diagram of the proposed RFG powering an inductive discharge

Since there is no need for high performance control of the RF power, a half-bridge consisting of the power semiconductors T_{+}, T_{-}, and the external free-wheeling diodes D_{+}, D_{-}, constitutes a good approach, as it allows the use of a simplified drive signal generation. In this configuration the RF power can be adapted by varying V_{DC}. Therefore, the capacitive intermediate circuit C_{DC}, in conjunction with the DC power supply used, needs to define an appropriate time constant. Using a full-bridge converter would result in higher output voltage and the ability of controlling the RF power via drive signal adjustment, however the complexity of drive signal generation and the required amount of silicon would increase.

Power semiconductors with short turn-on and turn-off times are essential to operate the converter in switching mode. Furthermore, switching frequencies above the desired output frequency are needed. Thus, for T_{+}, T_{-} only MOSFETs are applicable. The external free-wheeling diodes' forward voltage must be lower than the MOSFETs' body diodes' to provide sustainable switching-loss reduction. Likewise, a low reverse-recovery charge should be striven for.

The driver supply of the half-bridge is a crucial component. Since T_{+} forms a high-side switch, its reference potential floats according to the switching state of the half-bridge. To guarantee reliable decoupling between the drive levels of T_{+} and T_{-} and thus preventing cross-conducting, separated power supplies are used. Drive signals are transferred to the respective drive level via digital isolators.

The converter load needs to form a resonant circuit, to enable low-loss switching. Since the thruster coil—assisted by the plasma—forms an ohmic ($R_{\mathrm{c+pl}}$) and inductive ($L_{\mathrm{c+pl}}$) load, this can be achieved by adding a capacitor C_{res} in series. The capacitance is calculated depending on the desired output frequency f_0:

$$C_{\mathrm{res}} = \frac{1}{(2\pi f_0)^2 L_{\mathrm{c+pl}}} \quad (1)$$

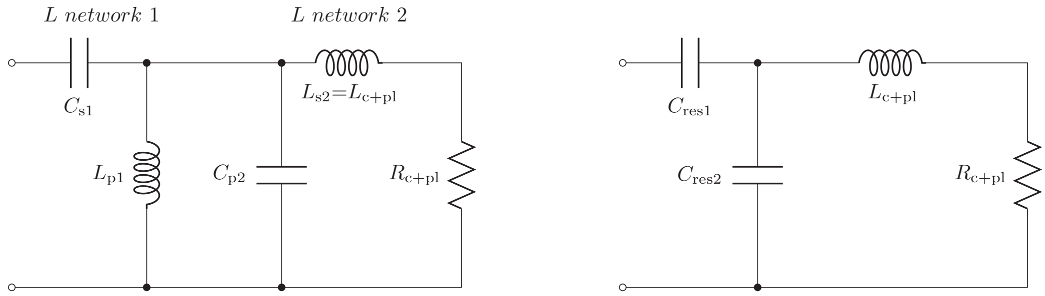

(a) T network for impedance transformation and quality improvement

(b) Simplified impedance transformation network

Figure 3. Impedance transformation network

Using the inductive load component to form a resonant circuit, the amount of required (lossy) components decreases and a compact assembly is feasible.

The series-resonant circuit is the simplest approach for realizing resonant switching behavior. However, by designing C_{res} only the RFG's output frequency can be adapted. To improve the overall efficiency, an impedance transformation of the thrusters' load component $R_{\text{c+pl}}$—which is typically low—is desired. This can be done by expanding the series-resonant circuit to an impedance transformation network. By using a T network, consisting of two L networks interconnected at their shunt legs as shown in Fig. 3(a), the coils' inductance $L_{\text{c+pl}}$ can advantageously be utilized and the overall load quality Q_{L} as well as the RF transfer efficiency can be increased. This arrangement can be simplified as shown in Fig. 3(b), resulting in just one additional capacitance parallel to the thruster coil for appropriate parameterizations. Corresponding design calculations are presented in Ref. 9. For optimal loss reduction, C_{res2} should be mounted as close as possible to the coil.

If the RF supply line is electrically short, no wave propagation and reflection phenomena will need to be considered.[10] To ensure this, the maximal length for a desired output frequency of 2.5 MHz is approximated by:

$$\begin{aligned} 2\,l_{\text{sl}} + l_{\text{coil}} &\overset{!}{\leq} \frac{\lambda_{\text{RF}}}{10} = \frac{v_{\text{RF}}}{10\ f_0} \approx \frac{\frac{2}{3}\ c}{10\ f_0} = 8\,\text{m} \\ l_{\text{sl}} &\overset{!}{\leq} 4\,\text{m} - l_{\text{coil}} \end{aligned} \tag{2}$$

Therefore, a short RF supply line—with its typical wave impedance of 50 Ω—does not produce radiation. Besides, it should be as short as possible to avoid wiring losses and ensure optimal energy flow into the thruster coil.

B. Control Concept

In general, the output power of resonant converters depends on the ratio of switching frequency f_{s} to resonant frequency f_0, achieving its maximum for $f_{\text{s}} \approx f_0$.[7] To maximize RF generation efficiency two facts need to be considered: output power must be maximized while switching losses must be minimized. Therefore, T_+ and T_- should be driven with respect to the resonant frequency f_0. Using a series-resonant circuit, f_0 can be determined by evaluation of the load current $I_{\text{Coil}} = I_{\text{Coil}}(t) = \text{Re}\{\tilde{I}_{\text{Coil}} \exp(\text{j}\omega t)\}$. Switching losses can be reduced by minimizing the current through the semiconductors during on- and off-switching operations. While operating the half-bridge with f_0, this can be achieved by switching near the zero crossings of I_{Coil}.

As changes of the plasma load affect both the equivalent series resistance $R_{\text{c+pl}}$ and inductance $L_{\text{c+pl}}$, they also influence the resonant frequency f_0. To ensure high output power while maintaining low switching losses, the switching frequency as well as the switch timing must be adjusted continuously. For this purpose, zero crossings of I_{Coil} are captured. Figure 4 shows a block diagram of the control loop.

The influence of the inductive discharge on $R_{\text{c+pl}}$ and $L_{\text{c+pl}}$ depends on inner plasma parameters as well as on the shape of the discharge vessel and the thruster coil. To estimate the modification of $R_{\text{c+pl}}$ and

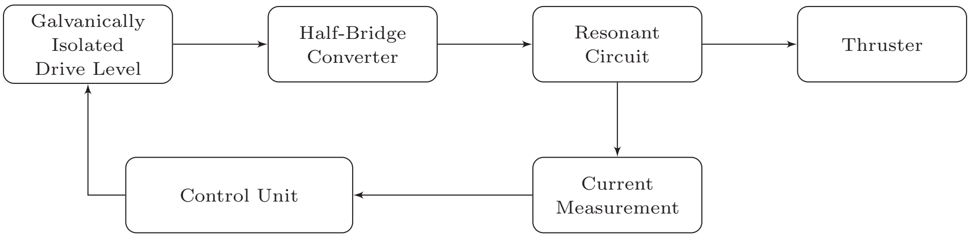

Figure 4. Block diagram of the control loop

L_{c+pl} for arbitrary RIT geometry and operating points, our research group has developed a self-consistent numerical model described in Ref. 4.

The current measurement provides a one-bit signal $i_{\text{zero}-\text{sig}}$, indicating whether the alternating load current I_{Coil} is positive or negative, as shown in Fig. 6. The edges of this signal correspond to the zero-crossings of I_{Coil}.

The control unit contains a specially developed frequency and phase regulation algorithm to provide the drive signals for T_+ and T_- according to the measurement signal $i_{\text{zero}-\text{sig}}$. Furthermore, it provides miscellaneous diagnostic and monitoring signals to maintain operational reliability.

For implementation, a new approach of a digital FPGA-based concept was chosen deliberately. So far, preferably analog control units have been used for time-critical applications such as the generation of gate control signals in the high frequency range. However, rapidly advancing developments of digital systems, make them increasingly operatable at higher clock speed and yield higher packing densities. As a result, digital systems gain more and more importance for use in time-critical applications. The key advantage of digital controllers is their high flexibility due to reconfigurable logic devices. Once functional changes of the control algorithm are required, they can easily be implemented by reprogramming. Analogues systems generally require a redesign in this case. Moreover, due to the high signal-to-noise ratio (SNR), digital systems provide improved accuracy and do not require periodic calibration. Besides, the communication with other systems can be realized fairly easy using predefined interfaces.

A FPGA basis was chosen due to its ability of generating precise control signals and high-speed data processing by parallelization. In contrast to micro-controllers (μC) or digital-signal-processors (DSP) their processing speed does not depend on the utilization rate and their computing power is not limited by the processor's word length, since the programmed algorithm is executed in hardware. In addition, they offer further advantages—which are crucial for space applications—such as low energy consumption and heat release as well as the ability of high radiation tolerance available by redundant design, enabled through cycle-synchronized processing.[11,12]

The block diagram of the control algorithm is shown in Fig. 5. For clarity, solely the generation of the drive signals is shown. In the first instance, the measurement signal $i_{\text{Zero}-\text{Sig}}$—indicating the sign of the load current I_{Coil}—is filtered to discard possibly occurring incorrect signal states due to EMI. Moreover, the input filter serves as a synchronization of the asynchronous input signal, which is very crucial for FPGA designs.[13] The edge detection block provides the edges of $i_{\text{Zero}-\text{Sig}}$, representing the zero-crossings of the load current. This signal fulfills two functions: it is used for periodic-time determination and drive signal generation.

The resonant frequency f_0 is identified by measuring the periodic-time of $i_{\text{Zero}-\text{Sig}}$. For this purpose, a binary counter—read out and reset by the positive edges of $i_{\text{Zero}-\text{Sig}}$—is implemented.

To ensure reliable operation, the switching frequency must be restricted. Therefore, the adjusting range of the switching periodic-time T_s is limited to predefined boundaries. If the detected periodic-time T_k exceeds those boundaries, it will be discarded and the last valid periodic-time will be passed on.

To put the RFG into operation, a start-up concept is essential since there is no oscillation in the resonant circuit at the beginning and thus $i_{\text{Zero}-\text{Sig}}$ delivers no measurement values. By activating the release signal *enable* the power-semiconductors are driven in open-loop mode with a constant periodic-time for a certain number of periods, until the current measurement provides valid data.

The drive signal generation is the centerpiece inside the control domain and contains the switching frequency-adapting algorithm. It is implemented using a finite state machine. The calculation of the power-semiconductor's conduction-time is done with respect to the determined periodic-time of I_{Coil} as well as

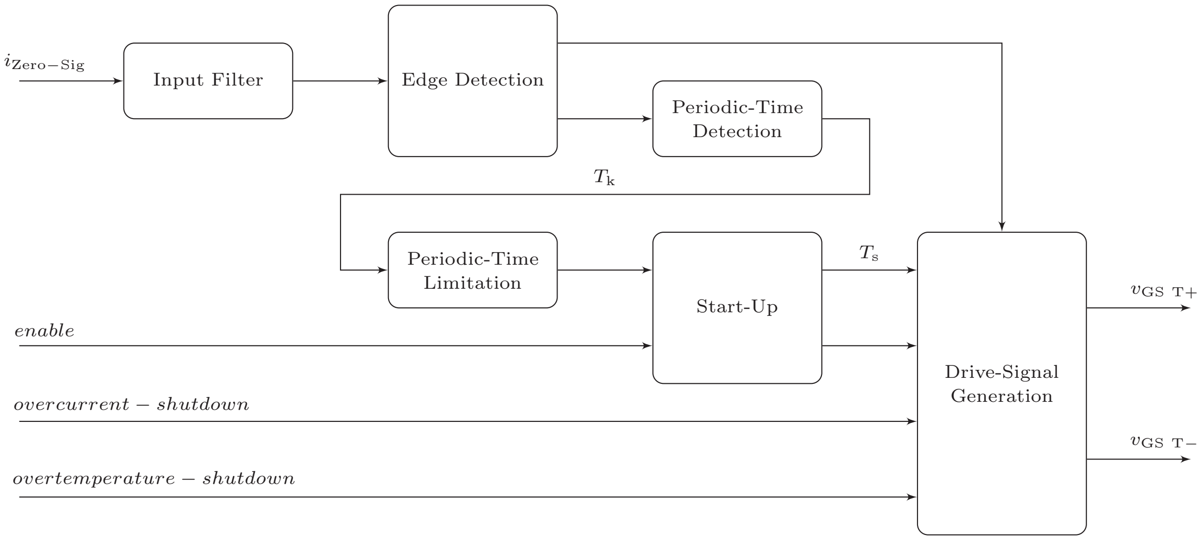

Figure 5. Block diagram of the control algorithm

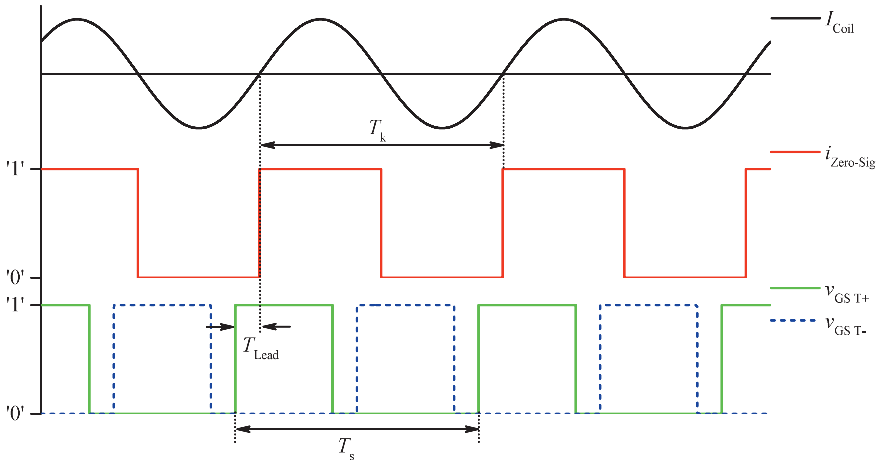

Figure 6. Control signals in steady state mode

its zero-crossings. The most effective operating point is reached when the resonant converter is operated in slightly over-resonant mode, which is due to the use of MOSFETs.[7] This is achieved by a very small reduction of the calculated conduction-times of T_+ and T_-. Moreover, each element of the control loop in Fig. 4 induces a dead time, depending on its propagation delay time. Thus, the overall performance as well as the maximum accessible switching frequency is limited. To guarantee low-loss switching, the dead time of the whole control loop must be compensated.

Figure 6 illustrates the control signals in steady state (constant resonance frequency f_0) with idealized current measurement. The signal $i_{\mathrm{Zero-Sig}}$ provides the sign and zero-crossing of I_{Coil}. This allows the determination of the periodic-time T_{k}, which serves for calculation of the switching periodic-time T_{s}. The edges in $i_{\mathrm{Zero-Sig}}$ are used for calculation of the conduction times. To prevent cross conducting, a locking-time component is inserted between the conduction states of T_+ and T_-. In addition, the dead time of the control loop is compensated by the lead time component T_{Lead}.

To ensure reliability, signals for overtemperature- and overcurrent-detection are added. By utilizing a second current sensor, the amplitude $\hat{I}_{\mathrm{Coil}}$ can be evaluated. For overload protection, the drive signal generation is put into idle mode if abnormal temperature on or current flow through the power semiconductors is detected.

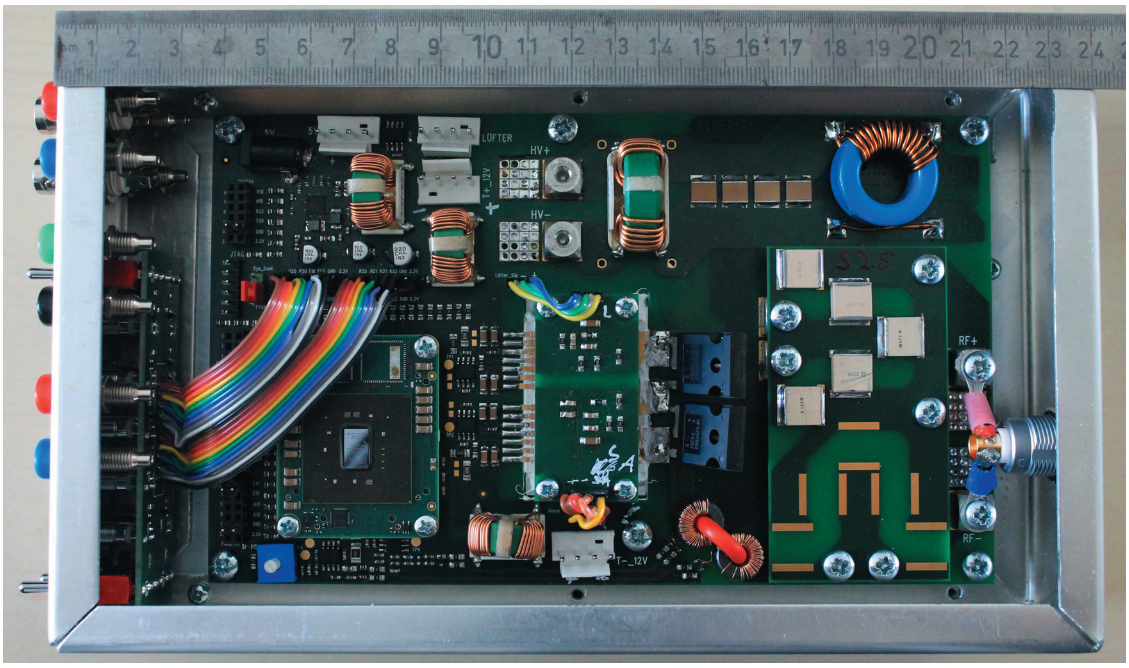

(a) Top view

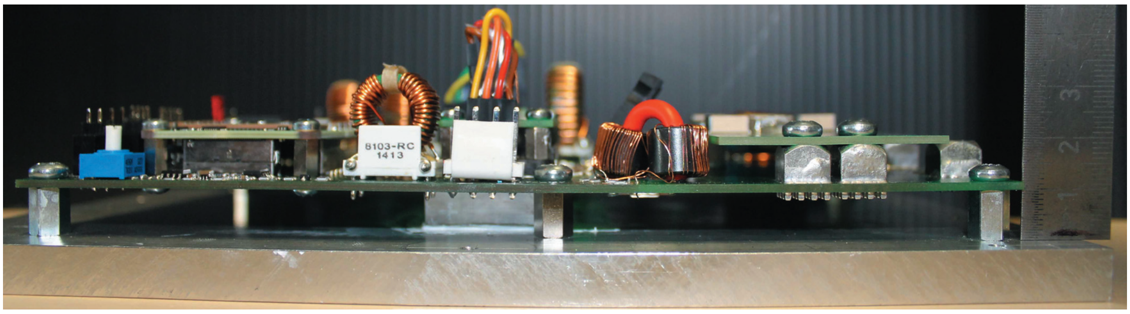

(b) Side view

Figure 7. RFG hardware assembly

III. Hardware Assembly and Measurement

To minimize cable losses, a mounting closely to the thruster is aspired. This is realized by a compact design. Figure 7 shows the hardware assembly of the RFG. Due to a four-layer assembly, small outline dimensions of 200 mm x 120 mm are feasible. A sufficient heat dissipation is crucial for the power semiconductors. Therefore, a massive base plate is connected to the MOSFETs' cases. Certain heat sinks can be mounted at its outer surface. For active cooling, a temperature dependent control signal is provided by the RFG's control unit. The adjustment of the resonance capacitors can easily be done by replacement since they are assembled on a dedicated board. For an improved overall efficiency, a shunt capacitance as shown in Fig. 3(b) is required. In case the mounting of C_{res2} closely to the thruster coil is not feasible, extra slots are provided on the RFG board. To minimize the impact of switching mode operation on the DC power supplies, common mode chokes are implemented in each supply line.

For verification of the RFG concept, a performance mapping is recorded when supplying a RIM-4 RF ion thruster, as shown in Fig. 8. The required RF power—calculated by multiplication of DC voltage and current—is plotted with respect to the volumetric xenon flow rate for a beam current of $I_{\mathrm{Beam}} = 5\,\mathrm{mA}$ and output frequencies of $\omega_{\mathrm{RF}} = 2, 2.5,$ and $3\,\mathrm{MHz}$. For an additional evaluation of the developed RFG concept, an equal performance mapping is done with an analog phase-locked loop (PLL) based RFG. Although the absolute values of required RF power depend on the laboratory setup, the two RFGs can be compared since

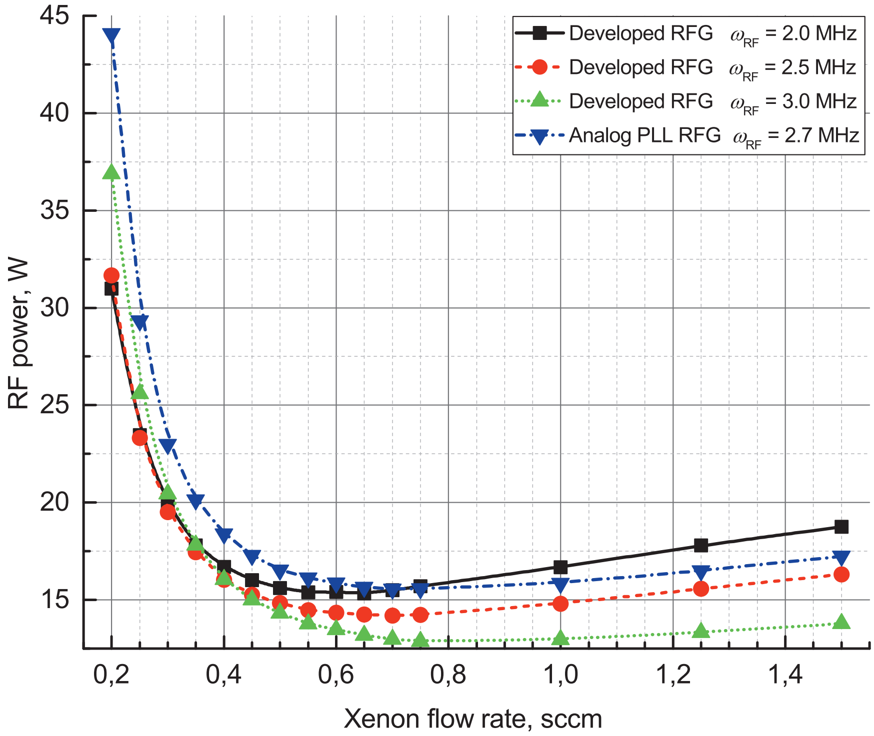

Figure 8. Performance mapping supplying a RIM-4 with $I_{\mathrm{Beam}} = 5\,\mathrm{mA}$

they both were driven within the same setup.

As can be seen in Fig. 8, with increasing frequency ω_{RF} the most efficient operating point slightly moves to higher flow rates. Furthermore, for operation on high flow rates greater frequencies generally require less input power. This is due to the rise of the electron-neutral collision frequency ν_{m}, since the optimum ω_{RF} is linearly dependent on ν_{m}. For low mass flows the choice of ω_{RF} is of secondary importance, which is due to the fact, that stochastic heating becomes increasingly important compared to ohmic heating within this region.

Compared to the analog PLL RFG, the developed RFG needs less RF power to maintain the requested beam current for typical flow rates below 0.6 sccm, regardless of the output frequency. For operation with a output frequency of $\omega_{\mathrm{RF}} = 3\,\mathrm{MHz}$ and a xenon flow rate of 0.75 sccm, the developed RFG is able to provide the same output power with 17 % less input power. Besides, auxiliary power consumption is not included, since it does not depend on the mass flow and, at the current state of development, the drive level supply of the developed RFG is not optimized for low power consumption.

IV. Conclusion and Outlook

In this paper, we have presented an efficiency-optimized RFG concept, operating in switching mode. By using a resonant-converter topology, resonant switching behavior can be established and thus, switching-losses can be minimized. To maintain resonant switching, an algorithm for frequency and phase-control is utilized, allowing an adjustment of RF-generation on altered load conditions within a few RF-cycles. By choosing a digital FPGA-based implementation of the control algorithm, high performance in tracking the maximum power point of operation is secured. Furthermore, the FPGA-implementation offers significant advantages such as low energy consumption and heat release—crucial for space applications.

Experimental studies have proven that the developed frequency and phase-control algorithm guarantees synchronized drive signal generation. The proper function of the designed hardware assembly was demonstrated through leadoff performance mappings supplying a RIM-4 RF ion thruster. Thus, the developed RFG concept can ensure successful operation of a RIT. In addition, by comparison to an analog phase-locked loop based RFG, the benefits of using a high efficiency, high performance RFG concept were shown.

To further increase the RF transfer efficiency—and thus minimize the required RF power for given flow rates—the series-resonant circuit should be replaced by an impedance transformation network, which is part of our ongoing work. Moreover, the drive level should be optimized for low power consumption, resulting in enhanced overall efficiency.

The developed RFG is used as a basis RF-supply concept for optimizing the RITs' overall efficiency and validate new thruster design concepts in our research group. To further improve the RFG concept, an investigation on evaluating the efficiency subject to the output frequency and beam current is part of our future work. In addition, an enhanced housing and optimized thermal management should be utilized, enabling long-lasting operation and ensuring safety and reliability.

References

[1]Brophy, J. R., "NASA's Deep Space 1 ion engine", *Review of Scientific Instruments*, Vol. 73, No. 2, 2002, p. 1071.

[2]Liebermann, M. A., and Lichtenberg, A. J., *Principles of Plasma Discharges and Materials Processing*, John Wiley & Sons, New Jersey, 2005.

[3]Loeb, H. W., "Radio Frequency Ion Sources for Electrostatic Propulsion (Hollow Cathode Design for Electron Bombardment Radio Frequency Ion Thruster Source)", *Proceedings of the Symposium on Ion Sources and Formation of Ion Beams*, 1971, pp. 77-84.

[4] Volkmar, C., Ricklefs, U., and Klar, P. "Self-Consistent Numerical 1D/3D Hybrid Modeling of Radio-Frequency Ion Thrusters", *Proceedings of the 34th International Electric Propulsion Conference*, ERPS, USA, 2015.

[5] Baruth, T., and Thüringer, R., "Radiated Emission Simulation of a RIT4", *Proceedings of the 34th International Electric Propulsion Conference*, ERPS, USA, 2015.

[6] Wolf, N., and Probst, U., "System Identification of a Radio-Frequency Ion Thruster", *Proceedings of the 34th International Electric Propulsion Conference*, ERPS, USA, 2015.

[7]Erickson, R. W., and Maksimović, D., *Fundamentals of Power Electronics*, 2nd ed., Kluwer Academic Pub., Massachusetts, USA, 2001, Chap. V.

[8]Chabert, P., and Braithwaite, N., *Physics of Radio-Frequency Plasmas*, 1nd ed., Cambridge University Press, New York City, USA, 2011, pp. 236.

[9]Bowick, C., Blyler, J., and Ajluni, C., *RF Circuit Design*, 2nd ed., Newnes (Imprint of Elsevier), Philadelphia, USA, 2007, Chap. 4.

[10]Pozar, D. M., *Microwave Engineering*, 3nd ed., John Wiley & Sons, New Jersey, USA, 2005.

[11]Ley, W., Wittmann, K., and Hallmann, W. (ed.), *Handbuch der Raumfahrttechnik*, 4nd ed., Hanser Verlag, Munich, Germany, 2011, pp. 372.

[12]Huber, F., Behr, P., Röser, H.-P., and Pletner, S., "FPGA Based On-Board Computer System for the "Flying Laptop" Micro-Satellite", *Proceedings of the Data System In Aerospace Conference*, SP 638, ESA, Netherlands, 2007.

[13]Altera Corporation (ed.), "Understanding Metastability in FPGAs", White-Paper-01082-1.2, San Jose, CA, 2009.